PEDOSPHERE（土壤圈英文版）

Pedosphere ISSN 1002-0160/CN 32-1315/P doi:10.1016/S1002-0160(21)60053-X

Development of a New Index for Automated Mapping of Ratoon Rice Cultivated Area using Time-series Normalized Difference Vegetation Index Imagery

NEW INDEX FOR AUTOMATED RATOON RICE MAPPING

Bolun LI[1], Shaobing PENG[2], Runping SHEN[1], Zong-Liang YANG[3], Xiaoyuan YAN[4], Xiaofeng LI[5], Rongrong LI[1], Chengye LI[1], and Guangbin ZHANG[4,*]

[1]*School of Geographical Sciences, Nanjing University of Information Science and Technology, Nanjing 210044 (China)*
[2]*College of Plant Science and Technology, Huazhong Agricultural University, Wuhan 430070 (China)*
[3]*Jackson School of Geosciences, The University of Texas at Austin, Austin (USA)*
[4]*Institute of Soil Science, Chinese Academy of Sciences, Nanjing 210008 (China)*
[5]*Northeast Institute of Geography and Agroecology, Chinese Academy of Sciences, Changchun 130102 (China)*

(Received 21 December, 2020; revised 20 July, 2021)

ABSTRACT

Over the past decades, the demand for food continues to grow worldwide due to population growth and the reduction of arable land. Rice ratooning offers new opportunities for raising rice production with limited labor input, which has renewed the interest in ratoon rice cultivation. Timely monitoring of the spatial pattern of both traditional and ratoon rice cultivations at regional scales is becoming essential information needed for studies of agricultural resource management and food security. However, similar phenological characteristics lead to poor separability between traditional double rice and ratoon rice systems from satellite observations. In this research, we first proposed an improved phenology-based rice detection algorithm using Moderate Resolution Imaging Spectroradiometer (MODIS) normalized difference vegetation index (NDVI) images. A new index was then developed for automatically delineating the ratoon rice paddy area with the aid of a readymade rice map in Hubei Province, China. The accuracy assessment using ground truth data showed that our approach could map both traditional and ratoon rice paddies with a high user accuracy (91.25% and 91.43%, respectively). Last, these MODIS retrieved rice areas were validated with annual agricultural statistic data, and R^2-values of 0.60 and 0.41 were recorded for traditional and ratoon rice paddies, respectively. The total planting area of ratoon rice in 2016 was estimated to be 1283.6 km^2 in Hubei Province, contributing 5.0% of the total rice paddy area. This work demonstrates the feasibility of extracting

*Corresponding author. E-mail: gbzhang@issas.ac.cn.

the spatial extent of both traditional and ratoon rice solely from time-series NDVI and field survey data. It makes strides towards routine monitoring traditional and ratoon rice distribution at the subnational level in timely ways. Given the historical satellite and phenology records, the proposed algorithms may have the potential to promote rice paddy mapping efforts across a broad temporal extent (1980s-present).

Key Words: area estimation, cross-correlogram, spectral matching, MODIS, NDVI, ratoon rice index

INTRODUCTION

Rice, the major staple for more than half of the global population, is at the heart of food security, as global rice production must be increased by 40% by the end of 2030 to meet the growing demand (OCDE, 2009). China is the leading rice producer in the world, accounting for 18.2% of the worldwide harvest area and 27.4% of the global production (FAOSTAT, http://www.fao.org/faostat/en/#data). Current self-sufficiency in rice production has been accomplished by increasing rice yields >30% since 1980 notwithstanding an 11% decrease in harvested rice area due to massive rural-to-urban demographic transition (Deng *et al.*, 2019). In recent years, land-use changes coupled with fast socio-economic development have strongly impacted rice production across the globe, particularly in China, where the rate of rice yield growth slowed distinctly. China would have to make strategic decisions for ensuring food security for 1.4 billion domestic people and other rice-reliant populations as well (Peng, 2014). A pressing need is to enhance yield without increasing the land area and, at less production cost per unit.

Rice ratooning offers an effective cultivation practice to achieve additional rice yields with minimal inputs (Harrell *et al.*, 2009). The ratoon rice is a second rice crop growing from the stubble left after the main rice harvest (Dong *et al.*, 2017). Global warming, to some extent, is considered to promote the cultivation of ratoon rice widely (Negalur *et al.*, 2017; Ziska *et al.*, 2018). Also, compared with the traditional rice systems (e.g., early rice, late rice, and middle rice), ratoon rice systems have the advantages of 50% lower production costs, 40% shorter growth duration, and higher water use efficiency (60% fewer water inputs) with 40–50% yield as that of main crop (Krishanamurthy, 1989; Santos *et al.*, 2003; Munda *et al.*, 2009). Therefore, shifting the traditional single rice system (just one main crop) into the ratoon rice system (main crop + ratoon crop) not only adapts to climate change but also represents a very large potential of increase in rice production.

Ratoon rice agriculture is currently distributed across the middle-lower Yangtze River region and Southern part of China (e.g., Hubei, Hunan, Sichuan, and Fujian provinces), with a continuously increasing planting area since the year 2011 (Peng, 2014). It is preliminarily estimated that the area of ratoon rice cultivation was over 8000 km^2 in 2018 (http://dy.163.com/v2/article/detail/EAJ4KJF0055004XG.html). But no nationwide statistical data on ratoon rice are publicly available in China yet. Furthermore, global warming may promote rice planting extending to the regions of 37 °N by the end of the 21st century (Ziska *et al.*, 2018), thus possibly causing the area of ratoon rice tended to increase greatly in the future (Nelson *et al.*, 2009). Therefore, timely monitoring of the area and cultivation practice in both traditional and ratoon rice systems is crucial for studying the effects of human activities and climate change on rice agriculture, as well as the influences of the area changes in rice paddy on the food security, economic development, biogeochemical cycles, and water resource management in China and worldwide (Matthews *et al.*, 1991; Olivier *et al.*, 1999; Leff *et al.*, 2004; Yan *et al.*, 2009; Li *et al.*, 2016).

Remote sensing technology, in combination with phenology data, has been widely used to acquire accurate spatial information for rice agriculture over large areas. Over the past few decades, the Moderate Resolution Imaging Spectrometer (MODIS) shows a good capability in providing daily and continuous data for land surface monitoring at different spatial scales, and a variety of MODIS-based algorithms have been designed for regional and continental mapping of rice paddies (Sakamoto *et al.*, 2005; Wardlow and Egbert, 2008; Lv and Liu, 2010; Wang and Lu, 2010; Chen *et al.*, 2011; Gumma *et al.*, 2011; Li *et al.*, 2020). These

approaches basically take advantage of a unique physical feature of the rice paddy surface because it is a mixture of soil, water and rice leaves during the transplanting stage but would be fully covered by rice crop canopy during the heading stage of the growing season. However, to our knowledge, few studies have investigated the spatial distribution mapping of ratoon rice with remotely sensed data. Deriving the ratoon rice coverage is methodologically challenging, mainly due to the phenological variations of ratoon rice canopy are quite similar to the traditional double rice (Yuan *et al.*, 2019). The difficulty of ratoon rice mapping arises largely from using either traditional statistics-based image classification techniques or phenology- and threshold-based segmentation algorithms.

With these issues in mind, the primary aim of this study is twofold: (1) To develop an automated phenology-based rice detection approach for large-scale application; and (2) To develop a new index for automatically delineating ratoon rice paddy area with the aid of a readymade rice map of 2016 in Hubei Province, China. To achieve these goals, in the first step, we used high-quality time-series MODIS normalized difference vegetation index (NDVI) data and spatial datasets of rice growth calendar to form NDVI difference images between key rice growth stages pixel by pixel. We then took advantage of the auto-thresholding method to recognize rice pixels from the NDVI difference images. Subsequently, we developed a new index based on the same time series NDVI dataset to automatically extract the ratoon rice area in Hubei Province. The proposed approaches (robust and automatic) can contribute to future efforts to update the annual geospatial database of rice cultivation and to support various studies of land-use and land-cover change, greenhouse gas estimations, and agricultural resource management.

MATERIALS

Study area

We selected Hubei Province, China (lying between 29°05′ N to 33°20′ N and 108°21′ E to 116°07′E) as the study area, where rice ratooning is well exemplified as an alternative of double rice cropping based on the traditional single rice (Fig. 1). The subtropical monsoon climate usually brings abundant precipitation and a long warm season. Annual mean temperature varies between 14 °C and 18 °C, while annual precipitation is normally concentrated in spring and summer, ranging from 1000 mm to 1500 mm. Single rice and double rice are the two main rice cropping systems adopted in Hubei Province. The annual rice-upland crop rotation system is dominant across the mid-west, where the landscape is generally flat with maximum elevations below 50 m. In the mid-east, a double-rice cropping system is commonly adopted, where the more hilly landscapes may result in more heterogeneous land cover types. Rice contributes a significant portion of the total arable area in Hubei, with approximately 22000 km^2 of area sown to paddy rice (NBS, 2016).

Fig. 1

Fig. 1 The spatial extent of Hubei Province and locations of sample sites.

MODIS satellite products

The MODIS 8-day composite gridded Surface Reflectance Product (MOD09Q1) of 2016 was used to calculate NDVI in this study. Each MOD09Q1 pixel value is the best quality observation during the 8-day composite period. MOD09Q1 data provide surface spectral reflectance of visible-red (VISR) and near-infrared (NIR) band at 250-m spatial resolution. The MODIS yearly Land Cover Type product (MCD12Q1) was adopted to create a non-rice mask of evergreen forests and stable water bodies to assist rice recognition. All of the MODIS datasets were downloaded from the USGS Land Processes Distributed Active Archive Center (http://lpdaac.usgs.gov) and reprojected to the WGS1984-UTM coordinate system (zone 49N).

Digital Elevation Model (DEM) data

To diminish the potential influence of the terrain factors on the estimate of rice area, a global 90-m raster SRTM void-filled elevation data was acquired from the USGS Global Visualization Viewer (GloVis) server (https://glovis.usgs.gov/). The slope data were calculated from the elevation data in the ENVI software (Exelis Visual Information Solutions, Boulder, CO, USA). Both the elevation and slope data were spatially aggregated to 250-m resolution.

Evaluation datasets

Two field surveys were conducted throughout the main rice planting areas from March 30 to April 14, 2017, and from October 6 to October 9, 2017, in Hubei Province. A total of 124 sample sites (including 40 ratoon rice samples, 45 traditional rice samples, and 39 non-rice samples), located with GPS, were set randomly distributed at approximately 5-km intervals. Additionally, high-resolution Google Earth imagery was commonly employed as a complementary source of ground truth dataset for coarse-resolution image classifications, owing to its availability for easy visual interpretation of the land cover (Beck, 2006; Knorn *et al.*, 2009; Dorais and Cardille, 2011; Peng *et al.*, 2011). We used the satellite images during the rice growing season of 2016 in Google Earth as the reference dataset. We then randomly collected 46 more non-rice samples from Google Earth images by visual interpretation around the rice paddy sites. In general, a total of 170 field sites were randomly selected across the rice planting area in Hubei Province as an evaluation dataset (Fig. 1).

Agricultural census data of ratoon rice planting areas in Hubei Province were provided by Huazhong Agricultural University and local agricultural agencies. They were compared with the remote sensing-derived results at the county level to assist in accuracy assessment.

METHODOLOGY

Reconstruction of time-series MODIS NDVI imagery

The cloud contamination appears particularly in the hilly area of mid-south China, thick clouds may obscure the land surface over a long time due to the monsoonal climatic conditions. To well capture the vegetation signals related to rice planting, the residual impact of persistent cloud cover in MOD09Q1 observations needs to be diminished before further analysis.

We used the Iterative Interpolation for Data Reconstruction (IDR) method to minimize the effects of cloud contaminations and construct high-quality NDVI time-series datasets throughout the year 2016. This approach was oriented towards removing the impacts of cloud contamination in the NDVI time series (Julien and Sobrino, 2010). The NDVI time-series profile is computed pixel by pixel from the preprocessed MOD09Q1 dataset. The mean NDVI value of the preceding and following observations is compared to the original NDVI for each time point. A replacement will be carried out when the maximum difference between the original and averaged time series is larger than the threshold (was set to 0.1 in this work suggested by Liu *et al.* (2017)). Then a new alternative time series is calculated from the averaged time series, and the process is iterated until the upper envelope of the NDVI time-series profile is reached. IDR has been shown to outperform the other commonly used methods (e.g. double logistic fitting) about the conservation of uncontaminated NDVI values (Julien and Sobrino, 2010). The main advantage of IDR is that it requires few parameter inputs and well conserves the upper envelope of the NDVI time-series profile (Sobrino and Julien, 2013). Since the temporal resolution of the original NDVI dataset was 8 days, the reconstructed time series was then temporally interpolated to daily scale for NDVI extractions in later procedures using a spline

interpolation function (White *et al.*, 2009). NDVI is computed from the VISR (620–670 nm) and NIR (841–875 nm) band surface reflectance values:

$$NDVI = \frac{NIR - VISR}{NIR + VISR} \quad (1)$$

Non-rice paddy mask

Firstly, to reduce the potential impacts of non-rice land-use types on rice paddy recognition, a mask of natural perennial plantation and permanent water bodies was necessary. We used the MCD12Q1 to generate non-rice paddy masks for separating water and evergreen forest from rice paddy pixels.

Secondly, although much of the rice cultivation in Hubei Province occurs in flat plains, there is some hilly landscape in the far west of the study area. This would pose challenges to the rice recognition process. Therefore, we adopted a regional terrain mask (Dem<1500 m & Slope<15°) from Li *et al.* (2020) to eliminate the potential influence of topography on the performance of the MODIS-based rice paddy recognition procedure.

Derivation of NDVI difference images between key rice growth stages

The Empirical Bayesian Kriging (EBK) interpolation method was adopted to achieve gridded spatial distribution of rice crop calendar information of the study area from the crop phenological observations at 211 agricultural meteorological stations (Supplementary Table S1 and Table S2), which were acquired from the China Meteorological Data Sharing Service System (http://data.cma.cn/data). The spatial resolution of the gridded interpolated rice calendar is 250 m. We used the Agro-phenological Atlas of China to correct and supplement the national site-based rice growth calendar (Zhang *et al.*, 1987). As a modern spatial interpolation algorithm, EBK has been applied in numerous recent studies in agricultural sciences (Samsonova *et al.*, 2017; Nocco *et al.*, 2019). The primary advantages of EBK over other conventional kriging methods include: 1) it enables both stationary and non-stationary local representations for the stochastic spatial process; 2) it automates the data transformation into a Gaussian distribution; 3) it automates the parameter calculations of building a valid kriging model; 4) it accounts for the model uncertainty in variable prediction; and 5) it can outperform the other kriging method with a relatively small dataset available (Krivoruchko, 2012; Gribov and Krivoruchko, 2020).

We further computed the corresponding NDVI difference (ΔNDVI) between the transplanting date and heading date pixel by pixel in terms of the spatial dataset of rice growth calendar:

$$\Delta NDVI = NDVI_{heading} - NDVI_{transplanting} \quad (2)$$

where $NDVI_{heading}$ and $NDVI_{transplanting}$ are the NDVI values for a given pixel of the heading and transplanting date, respectively.

Mapping traditional and ratoon rice paddies

Fig. 2 provides a schematic workflow of the MODIS-based rice/ratoon rice identification approach. The changes of NDVI between rice transplanting and heading stage on the MODIS images were used to map rice areas. We used a gridded rice crop calendar to choose the corresponding NDVI value from the time-series remote sensing imagery pixel by pixel a priori for rice detection. Based on the derived overall

rice map, we developed a ratoon rice index (RRI) to automatically detect ratoon rice pixels from the NDVI time series.

Fig. 2

Fig. 2 Schematic workflow of the traditional and ratoon rice detection based on MODIS data. RRI: ratoon rice index. ΔNDVI: the NDVI difference between the transplanting stage and heading stage.

Methodology for identifying rice paddy. The major challenge for differentiating rice from other upland crops (e.g., corn) is to detect their phenological divergences. Transplanting is a unique growth stage to rice cultivation. During a single rice growing season, the vegetation index (VI) value usually reaches a low point at the flooding and transplanting stage due to the coverage by a mixture of rice leaves and water over the paddy surface, and it rises to a high point and peaks at the heading stage (the end of reproductive phase) when the vegetation signal dominates the paddy surface (Peng *et al.*, 2011; Li *et al.*, 2020). It makes the NDVI differentiation during this period of rice should be larger than other crop types (see the RESULTS section). To guarantee the simplicity and maximize the generalization of the algorithm, we introduced NDVI as the only remote sensing index in the formulations.

As the NDVI difference between the transplanting stage and heading stage is expected to reach or approximate the maximum during the growing season, two NDVI tiles were collected for Hubei Province based on the derived spatial dataset of rice growth calendar pixel by pixel. One NDVI tile was on the transplanting date, and the second was on the heading date. Last, we synergistically performed image differencing and segmentation on the two-date NDVI tiles during the rice growing season to map the rice paddy distribution.

Li *et al.* (2020) developed a robust phenology-based approach to map rice paddies in China using the MOD09Q1 data. An Otsu's algorithm-based auto-thresholding process was introduced to track those image pixels that experienced a relatively larger change in NDVI from transplanting to heading stage (Otsu, 1979), which would be recognized as rice pixels. Notwithstanding Otsu's method was able to obtain fairly good classification results, it still fell prey to some flaws. First, original NDVI images of transplanting and heading date were directly used based on the mean date of the stationary rice growth calendar. The NDVI variation may not be well captured at the county level. Second, Otsu's method usually fails to approximate the accurate NDVI threshold where the rice paddy accounts for a relatively small fraction of the landscape because the assumption of a bimodal histogram distribution would be violated (Kittler and Illingworth, 1985).

To better differentiate rice from the other land use categories under various fractional cover of rice cultivation, we used an integral image-based adaptive thresholding algorithm to automatically determine the threshold for the NDVI difference image segmentation. The adaptive thresholding method employed here not only accounted for spatial variations in illumination but also was robust to illumination or other problems in the image. An integral image was calculated from the ΔNDVI over overlapped predefined rectangular windows in constant time. Then, a flexible threshold value (local average of the integral image) was assigned to each image pixel. Finally, a peak-valley detection algorithm was adopted to automatically find dominant peaks and valleys of the achieved threshold image histogram (Silva *et al.*, 2010). The maximum threshold ($T_{\max}$) of "valleys" was determined for pixel-wise rice identification (Fig. 3):

$$Class_{i,j} = \begin{cases} \text{Rice}, & \Delta NDVI \geq T_{\max} \\ \text{Non-rice}, & \Delta NDVI < T_{\max} \end{cases} \quad (3)$$

A detailed description of the adaptive thresholding method and data processing can be found in Bradley and Roth (2007). We conducted radiometric normalization before the image segmentation in the ENVI software to further minimize radiometric differences between two images caused by changes in atmospheric and illumination conditions (Canty, 2014).

Fig. 3

Fig. 3 Histogram of ΔNDVI threshold values within (a) early rice, (b) late rice, and (c) middle rice growth period in Hubei (red dashed line position is the determined threshold for rice pixels).

Methodology for identifying ratoon rice paddy. Cross-correlogram spectral matching (CCSM) is a widely used method for key absorption feature matching. It constructs cross-correlograms between a target and a reference spectrum at different match positions towards quantifying the corresponding similarities at a key absorption feature (Van Der Meer and Bakker, 1997; van der Meero and Bakker, 1997). As an extension of CCSM, Chen *et al.* (2016) proposed a weighted cross-correlogram spectral matching (WCCSM) algorithm to detect phenological change with time-series VI data. To implement the WCCSM method, the VI time-series profiles of the reference and target years are consequently taken as the reference and target spectrum. Different weights were assigned to different time points in the temporal segment in order to capture the subtle shifts to a reference phenological point on the reference VI time-series profile. Then, the weighted correlation coefficient ($R_{w,m}$) is computed between the pairwise VI time-series profiles from the target year/pixel and the reference year/pixel at different match positions (m). While the reference VI time-series profile is fixed, the match position refers to the temporal shifts with the target year/pixel data to calculate correlation coefficients.

Phenological differences between traditional double rice and ratoon rice crops are relatively small and only occur within a short time window around the harvest date of the main season (HD_{main}) on the reference NDVI profile. The key to distinguishing ratoon rice from other rice cropping systems is the timing of harvest of the main season. WCCSM has demonstrated its advantages as being sensitive to the shape of targeted NDVI profile features but insensitive to noise (Chen *et al.*, 2016). Therefore, based on the WCCSM method, we designed a new ratoon rice index (RRI) to provide an effective and robust method to enhance ratoon rice presence in remotely sensed imagery. The basic idea is to calculate the similarity between the pairwise NDVI time-series profiles from a target pixel and the reference ratoon rice pixel in a specific year. First, the weight w_i of each chosen point on the NDVI profile is set as decreasing with the temporal distance D_i between the date t_i and the reference HD_{main} date t_r (day 232) as below:

$$D_i = \begin{cases} 1, & t_i = t_r \\ \dfrac{1}{(t_i - t_r)^2}, & t_i \neq t_r \end{cases} \tag{4}$$

$$w_i = \frac{D_i}{\sum_{i=1}^{n} D_i} \tag{5}$$

where n is the number of overlapped days between the reference and the target time-series profile, and t_r is determined from the reference profile. Then, the correlation coefficient (R_m) and weighted cross-correlation coefficient ($R_{w,m}$) are calculated between the selected segment of the NDVI time-series profile in the target profile and its counterpart in the reference profile (see the RESULTS section) at different match positions (m) as:

$$R_m = \frac{\sum_{i=1}^{n}\left(VI_{t,i} - \overline{VI_t}\right)\left(VI_{r,i} - \overline{VI_r}\right)}{\sqrt{\left[\sum_{i=1}^{n}\left(VI_{t,i} - \overline{VI_t}\right)^2\right]\left[\sum_{i=1}^{n}\left(VI_{r,i} - \overline{VI_r}\right)^2\right]}} \tag{6}$$

$$R_{w,m}=\frac{\sum_{i=1}^{n} w_i\left(VI_{t,i}-\overline{VI}_t^{w}\right)\left(VI_{r,i}-\overline{VI}_r^{w}\right)}{\sqrt{\left[\sum_{i=1}^{n} w_i\left(VI_{t,i}-\overline{VI}_t^{w}\right)^2\right]\left[\sum_{i=1}^{n} w_i\left(VI_{r,i}-\overline{VI}_r^{w}\right)^2\right]}} \tag{7}$$

where w_i is the weight of the ith overlapped point in both the reference and the target profile, and $VI_{r,i}$ and $VI_{t,i}$ are the NDVI values on the ith overlapped day of the reference time-series profile and target time-series profile, respectively. $\overline{VI}_r$ and $\overline{VI}_t$ are the mean NDVI values of the reference and target profile segments, whereas $\overline{VI}_r^{w}$ and $\overline{VI}_t^{w}$ are the weighted mean NDVI values of the reference and target profile segments, respectively. Then, the cross-correlogram and weighted cross-correlogram are constructed pixel-wise by plotting R_m and $R_{w,m}$ against the corresponding m. We further determine a negative match position if the target-pixel profile is shifted to an earlier date and a positive match position if it is shifted to a later date. As a result, a "0" match position implies a direct calculation of the initial/weighted correlation between the target and reference profiles, whereas the match position "1" implies that the NDVI time-series profile for the target pixel will be shifted by one day in a later temporal direction.

The ratoon rice requires a specific and precise period for the harvest stage. According to the field survey, usually, the ratoon rice across the whole study area needs to be harvested within one month, since the ratoon season growth is mainly controlled by temperature in this stage (Yuan *et al.*, 2019). Thus, we set the match position m in a range from −15 to 15 days for the cross-correlation computation. The perfect matching situation is that there is no temporal shift ($m = 0$) between the reference and target time-series profile either for cross-correlogram or weighted cross-correlogram. Then, the RRI to enlarge local discrepancies of the harvest date of the main rice crop between ratoon rice and other traditional rice systems were developed as:

$$RRI=\begin{cases}\max\left\{R_{w,m}\right\}\times\max\left\{R_m\right\}\times\left(1-\dfrac{\left|m_{w,p}-m_p\right|}{\left|m_{w,p}\right|+\left|m_p\right|}\right), & \left|m_{w,p}\right|\le 15\\ 0, & \left|m_{w,p}\right|>15\end{cases} \tag{8}$$

where RRI is ratoon rice index, and m_p and $m_{w,p}$ are the optimal match positions with the maximum cross-correlation coefficient and weighted cross-correlation coefficient in the cross-correlogram, respectively. Match position m is set in a range from −15 to 15 days. After obtaining the maximum correlation (R_{max}) and weighted maximum correlation ($R_{w,\,max}$), their significance is assessed using the t-test. If R_{max}/$R_{w,\,max}$ cannot pass the significance test, it is set as 0. Otherwise, the value shall be retained.

The reference profile is the "averaged" NDVI profile between representative samples of ratoon rice from different geographic regions of the study area (see the RESULTS section). The generalized procrustes analysis (GPA) derived ensemble average NDVI time-series profile of five representative ratoon rice samples (from the northern, southern, western, eastern, and central part of Hubei, respectively), covered by homogeneous 250-m pixels, was adopted as the reference profile partly because the phenological date of ratoon rice varies slightly across Hubei. Finally, we again used the adaptive thresholding method to extract the spatial extent of ratoon rice from the RRI map. Detailed descriptions of the GPA algorithms are available in the work of Gower (1975) and Li *et al.* (2016).

RESULTS

NDVI images of key rice growth stages

Fig. 4 showed the reconstructed NDVI temporal profiles throughout 2016 at the representative rice crop pixels. During the rice growing season, the NDVI profiles of different rice crops were all found to reach a low point around the flooding and transplanting stage, constantly increased afterward, and peaked approximately at the end of the reproductive phase (heading stage). These results also corroborate the findings of previous studies (Xiao *et al.*, 2005; Peng *et al.*, 2011). Except for double cropping rice, large phenological discrepancies were found in the NDVI profiles between ratoon rice and other non-ratoon rice crops. The spatial distribution of transplanting date and heading date in 2012 were achieved respectively for early, late and middle rice using the EBK method (Supplementary Fig. S1). The general spatial variation of transplanting date and heading date was similar except for late rice. For early rice, both the transplanting date and heading date increased along the south-east to north-west direction, while the middle rice showed an opposite pattern. The late rice cultivation in the northeast part of Hubei Province had a relatively shorter growth period in contrast to both early and middle rice. Moreover, the variation range of both transplanting and heading date of middle rice reached 37 and 21 days, respectively, which were much larger than those of early and late rice. The corresponding NDVI images of transplanting date and heading date were then achieved based on the spatial dataset of the rice growth calendar (Supplementary Fig. S2).

Fig. 4

Fig. 4 NDVI time series of single rice, double rice, ratoon rice, and upland crop in Hubei Province (during ratoon rice growth period).

Spatial patterns of rice paddies

The resulting maps of 2016 illustrate that the spatial distributions of middle rice, early rice, and late rice derived from the adaptive thresholding method and Otsu's method share a similar pattern (Fig. 5). Specifically, double rice crops were concentrated along the Yangtze River, the Han River, and the south-west hilly regions, while middle rice crops mainly occurred around the Yangtze River, the Han River, and Nanyang Basin regions, where the irrigation condition and topography were suitable for rice growth (Fig. 1). Late rice agriculture was more fragmented as hilly regions dominate in most of those areas, increased altitude and slope may restrain the appearance of rice crops.

Fig. 5

Fig. 5 Spatial patterns of (a) early, (b) late, and (c) middle rice derived from adaptive thresholding method and (d) early, (e) late, and (f) middle rice derived from Otsu's method in Hubei of 2016.

However, there are still evident regional discrepancies between the spatial datasets derived from the two methods. The derived paddy areas were 23974.0, 31141.6, and 3541.6 km^2 for middle, early, and late rice based on Otsu's method, respectively, while the adaptive thresholding method yielded areas of 10735.3, 11815.4, and 4347.6 km^2 for middle, early, and late rice, respectively. Otsu's method produced notably larger rice planting areas than the adaptive thresholding method for both early and middle rice crops. For early rice, the adaptive thresholding-based method identified more rice paddies in central Hubei but less of that in the Dongting Lake region compared to Otsu's method. For late rice, this method has higher fractional amounts in the Dongting Lake region but lower fractional amounts in Northeast Hubei.

Reference NDVI time-series profile for ratoon rice

To implement the CCSM and WCCSM algorithms, an NDVI time-series profile of ratoon rice growing season (around day 140–290) is required as a reference profile. We then compared the pixel-wise NDVI time-series profile within the study area with the reference profile to build a cross-correlogram at different match positions. Since we only utilized five selected samples to construct the reference profile (Fig. 6), this could further evaluate the robustness and efficiency of the method.

Fig. 6

Fig. 6 Reference NDVI profile (red line) derived from representative ratoon rice sample sites (black lines). S_n: the n^{th} representative ratoon rice sample.

Spatial pattern of ratoon rice

We mosaicked the derived rice paddy maps from all of the rice crop systems. The mosaicked rice map consequently included both traditional and ratoon rice areas. We calculated the RRI of Hubei in 2016 (Supplementary Fig. S3) within the rice area. The spatial pattern of ratoon rice was then extracted based on the adaptive thresholding method (Fig. 7). The ratoon rice crop was mainly distributed in the center-south and eastern parts of Hubei Province, which was 1283.6 km^2, or responsible for 5.0% of the total rice paddy area.

Fig. 7

Fig. 7 Spatial pattern of ratoon rice in Hubei of 2016.

Accuracy evaluation of rice paddy map

The accuracies of the mosaicked rice map were subsequently accessed using confusion matrices calculated based on the 170 ground-truth samples. As can be seen from Table I, the overall accuracies for adaptive thresholding and Otsu's methods were 88.82% and 80.00%, respectively. The rice class of adaptive thresholding had a higher producer and user accuracy (85.88% and 91.25%) than that of Otsu's method (83.53% and 78.02%). The relatively higher Kappa coefficient was for adaptive thresholding (0.78) in comparison to Otsu's method (0.60).

TABLE I

The comparison of classification accuracies of rice paddy maps in 2016 derived from the Otsu-based method and method proposed in this study.

Method	**Ground truth (Pixels)**		**Total**
	Class	**Rice**	**Non-rice**

	Rice	71	20	91
	Non-rice	14	65	79
	Total	85	85	170
Otsu-based	Prod. Acc. (%)	83.53	76.47	
	User Acc. (%)	78.02	82.28	
	Overall accuracy (%)	80.00%		
	Kappa coefficient	0.60		
	Rice	73	7	80
	Non-rice	12	78	90
	Total	85	85	170
This study	Prod. Acc. (%)	85.88	91.76	
	User Acc. (%)	91.25	86.67	
	Overall accuracy (%)	88.82%		
	Kappa coefficient	0.78		

As an ancillary approach to the field survey, we compared the MODIS-derived rice paddy maps with the agricultural census data at the county level (Fig. 8). The R^2 between the MODIS-derived data and the statistical data was 0.60 and 0.51 based on the adaptive thresholding method and Otsu's method, respectively. Both correlations were significant at the level of $P < 0.001$ ($n = 78$). The RMSE between them was 265.2 and 745.4 km^2, respectively.

Fig. 8

Fig. 8 County-level evaluation of rice paddy area estimation based on (a) adaptive thresholding method and (b) Otsu's method against agricultural census data in Hubei of 2016.

Thus, it can be concluded that either method can produce a substantial agreement between the rice maps and ground truth data (Landis and Koch, 1977). The adaptive thresholding method performs relatively better in correctly predicting rice paddies than Otsu's one, especially for the early rice class, and showed higher consistency with the agricultural census data.

Accuracy evaluation of ratoon rice paddy map

The pixel-wise RRI was calculated using Eq. (8), the threshold was then determined also using the adaptive thresholding algorithm. We evaluated the MODIS-derived ratoon rice map based on the 170 ground-truth samples, and the confusion matrix is shown in Table II. The ratoon rice map had a fairly high producer accuracy (80%) and user accuracy (91.43%), while the omission and commission errors were 20% and 8.57%, respectively. The overall accuracy was 93.53%, and the Kappa coefficient was 0.81, indicating that the ratoon rice map corresponded well with the ground reference data.

TABLE Ⅱ

The classification accuracy of ratoon rice paddy map in 2016.

Ground truth (Pixels)	**Hubei**		**Total**
Class	**Ratoon rice**	**Non-ratoon rice**	
Ratoon rice	32	3	35

Non-ratoon rice	8	127	135
Total	40	130	170
Prod. Acc. (%)	80.00	97.69	
User Acc. (%)	91.43	94.07	
Overall accuracy (%)	93.53%		
Kappa coefficient	0.81		

Fig. 9

Fig. 9 County-level evaluation of ratoon rice area estimation against agricultural census data in Hubei of 2016.

We also compared our MODIS-derived ratoon rice paddy map with the census data at the county level (Fig. 9). The MODIS-derived estimates of the ratoon rice area are analogous to the reported census data. and their correlation was significant at the level of $P < 0.001$ ($n = 17$). The results corroborated the feasibility of applying RRI for mapping the ratoon rice area.

DISCUSSION

Improvement of phenology-based rice mapping approaches

Unlike other phenology-based classification approaches, which combine different vegetation indices that are sensitive to the changes of rice canopy and land surface water content (e.g., NDVI, EVI and Land Surface Water Index) (Xiao *et al.*, 2005; Xiao *et al.*, 2006; Peng *et al.*, 2011; Kontgis *et al.*, 2015), our method simply uses NDVI. This considerably reduces the computational cost and increases the generalizability of the method without compromising accuracy. It is, therefore, feasible to apply this method to the satellite sensor designed without a visible-blue (VISB) or shortwave-infrared (SWIR) band (e.g., NOAA AVHRR). Our method would facilitate the extension of rice paddy mapping efforts back to the 1980s with the historical satellite record. The evaluation results indicate that the single VI-based method has the potential to accurately map different rice cropping systems. Compared to other recently developed MODIS-based rice mapping methods, our method shows a comparable or higher mapping accuracy in China (Zhang *et al.*, 2015; Liu *et al.*, 2020).

As an improvement and extension of our previous effort in China (Li *et al.*, 2020), this study significantly improve the accuracy of rice mapping. For both methods, the key aspect is to implement a binary classification on ΔNDVI images. Several factors could be responsible for the improvement of this study. On the one hand, the adaptive local thresholding method can capture more details of the NDVI variations between key rice growth stages (rice transplanting-heading period) under non-uniform illumination in the mosaicked MODIS 8-day composite data (Bradley and Roth, 2007), then alternative local ΔNDVI thresholds were selected pixel by pixel. This method was thus capable of reflecting the slight discrepancies of ΔNDVI among different land cover types well but insensitive to the residual bias after atmospheric corrections. Based on that, the peak-valley detection algorithm determined a more precise threshold for final ΔNDVI image segmentation rather than directly using Otsu's method. However, Otsu's method tended to overestimate the rice paddy areas because the global ΔNDVI thresholding often fails if some other vegetation types were having similar phenological patterns (Fig. 4), or the atmospheric condition varies spatially within the daily MODIS images mosaiced from different tiles. Then it would easily form monomodal histogram distributions by the target image pixels, which go against the original assumption of a bimodal histogram distribution (Supplementary Fig. S4). On the other hand, the proposed method uses an ΔNDVI image derived from the gridded rice growth calendar rather than a mean date of the stationary rice growth calendar. Although the rice growth phenology remains relatively stable throughout Hubei Province for double rice crops, the sub-regional disparities in transplanting and heading date can exceed 20 days for

middle rice, partly due to the farmer's choice and/or meteorological condition (Supplementary Fig. S1). Using a fixed rice growth calendar for the whole study area would certainly bring bias in creating the ΔNDVI image. Notwithstanding these advances, our approach is largely dependent upon the local rice growth calendar data, the lack of continuous and timely rice spatial phenological datasets may somewhat hinder the application of this method. A future study hence should be carried out to establish time-series geospatial databases of rice growth calendar for China using a remote sensing approach.

Strengths and limitations of RRI

Ratoon rice identification largely relies on the short time window of harvesting of the main rice crop. The data availability can limit the use of single-date image classification methods in persistently cloudy areas (e.g., monsoon Asia). In this research, we developed a strategy to map ratoon rice areas automatically from reconstructed time-series NDVI data. The newly proposed RRI was found to be feasible by dramatically enlarging the phenological difference between ratoon rice and the other rice cropping systems based on their unique phenological characteristics. After masking out the non-rice areas based on a readymade rice map, the adaptive thresholding method was once again employed to automatically identify ratoon rice from the RRI map. The performance of the method has been examined using ground surveys and agricultural census data. The high overall accuracy (93.53%) and Kappa coefficient (0.81) demonstrated that the reference VI profile could be reliably derived from very few sample sites, probably because the ratoon rice growth calendars are much the same in Hubei Province (a specific region). The RRI could effectively produce accurate ratoon rice maps with an automatic threshold section.

Several caveats regarding the limitations of the regional mapping for ratoon rice using RRI should be addressed. First, as mentioned above, a high-quality reference VI profile of ratoon rice is required before calculating RRI. It relies on ground surveys for precise sample site locations because it is very difficult to directly visually interpret ratoon rice from other rice cropping systems even using high-resolution satellite imagery. Second, a readymade rice base map is also needed to exclude the influence of other crop types prior to extracting ratoon rice, although there are already a few continental-scale products available in the public domain.

The consistency between the MODIS-derived and statistical agricultural data of traditional rice systems was distinctly lower than that of ratoon rice. The likely causes may be associated with two aspects. First, compared to the official agricultural census, the ratoon rice area statistics provided by Huazhong Agricultural University and local agricultural agencies could be more biased due to policy impacts and lack of rigorous data quality control (Smil, 1999; Frolking *et al.*, 2002). Second, the producer accuracy of the ratoon rice map (80.00%) was markedly increased after the exclusion of misclassified total rice sites (88.89%, Supplementary Table S3). This implied that the accuracy of the rice base map can have a direct impact on the ratoon rice extraction result.

CONCLUSIONS

This study showed that the spatial pattern of multiple rice cropping systems including ratoon rice can be mapped accurately at a large scale with only time-series MODIS NDVI imagery and phenology information. With the aid of spatial database of the rice growth calendar, NDVI tiles of the key rice growth stages (transplanting and heading stages) were well reconstructed, which could capture the difference between the two key rice growth stages more precisely. In conjunction with the automatic image thresholding procedure, the NDVI difference image was optimally segmented to characterize the pixels as 'rice' or 'non-rice'. Then, a new index - RRI for automatically mapping ratoon rice was proposed based on the readymade rice map. To our knowledge, the mapping approach for the alternative rice cropping system-ratoon rice was explored based on MODIS data for the first time. Good linear relationships were obtained between the satellite-derived result and the agricultural census data for both traditional rice and ratoon rice crops. Compared to the previous MODIS-based rice mapping algorithm, this improved algorithm can produce more accurate rice paddy cover maps of traditional single and double rice crops separately. The

proposed strategy can also be extended to other time-series multi-spectral remotely sensed data without a VISB or SWIR band for mapping multiple rice cropping systems across a much broader temporal extent.

ACKNOWLEDGMENTS

This research was funded by the Youth Innovation Promotion Association of Chinese Academy of Sciences (2018349), the Startup Foundation for Introducing Talent of Nanjing University of Information Science and Technology (2016r036), the Innovation and Entrepreneurship Training Program Project for the Jiangsu College Students (2017103000165), the Strategic Priority Research Program of the Chinese Academy of Sciences (XDA05020200), and the National Natural Science Foundation of China (91437220).

SUPPLEMENTARY MATERIAL

Supplementary material for this article can be found in the online version.

REFERENCES

Beck A. 2006. Google earth and world wind: Remote sensing for the masses. *Antiquity.* **80**.

Bradley D, Roth G. 2007. Adaptive thresholding using the integral image. *J Graph Tools.* **12**: 13-21.

Canty M J. 2014. Image analysis, classification and change detection in remote sensing: With algorithms for envi/idl and python. Crc Press.

Chen C-F, Son N-T, Chang L-Y, Chen C-C. 2011. Monitoring of soil moisture variability in relation to rice cropping systems in the vietnamese mekong delta using modis data. *Appl Geogr.* **31**: 463-475.

Chen J, Rao Y, Shen M, Wang C, Zhou Y, Ma L, Tang Y, Yang X. 2016. A simple method for detecting phenological change from time series of vegetation index. *IEEE Trans Geosci Remote Sens.* **54**: 3436-3449.

Deng N, Grassini P, Yang H, Huang J, Cassman K G, Peng S. 2019. Closing yield gaps for rice self-sufficiency in china. *Nat Commun.* **10**: 1725.

Dong H, Chen Q, Wang W, Peng S, Huang J, Cui K, Nie L. 2017. The growth and yield of a wet-seeded rice-ratoon rice system in central china. *Field Crops Res.* **208**: 55-59.

Dorais A, Cardille J. 2011. Strategies for incorporating high-resolution google earth databases to guide and validate classifications: Understanding deforestation in borneo. *Remote Sens.* **3**: 1157.

Frolking S, Qiu J, Boles S, Xiao X, Liu J, Zhuang Y, Li C, Qin X. 2002. Combining remote sensing and ground census data to develop new maps of the distribution of rice agriculture in china. *Global Biogeochem Cycles.* **16**: 1091.

Gower J C. 1975. Generalized procrustes analysis. *Psychometrika.* **40**: 33-51.

Gribov A, Krivoruchko K. 2020. Empirical bayesian kriging implementation and usage. *ScTEn.* **722**: 137290.

Gumma M K, Nelson A, Thenkabail P S, Singh A N. 2011. Mapping rice areas of south asia using modis multitemporal data. *APPRES.* **5**: 053547-053547-053526.

Harrell D L, Bond J A, Blanche S. 2009. Evaluation of main-crop stubble height on ratoon rice growth and development. *Field Crops Res.* **114**: 396-403.

Julien Y, Sobrino J A. 2010. Comparison of cloud-reconstruction methods for time series of composite ndvi data. *Remote Sens Environ.* **114**: 618-625.

Kittler J, Illingworth J. 1985. On threshold selection using clustering criteria. *Systems, Man and Cybernetics, IEEE Transactions on.* 652-655.

Knorn J, Rabe A, Radeloff V C, Kuemmerle T, Kozak J, Hostert P. 2009. Land cover mapping of large areas using chain classification of neighboring landsat satellite images. *Remote Sens Environ.* **113**: 957-964.

Kontgis C, Schneider A, Ozdogan M. 2015. Mapping rice paddy extent and intensification in the vietnamese mekong river delta with dense time stacks of landsat data. *Remote Sens Environ.* **169**: 255-269.

Krishanamurthy K. 1989. Rice ratooning as an alternative to double cropping in tropical asia. *In* Rice Ratooning,, Bangalore (India), 1989. IRRI, pp.

Krivoruchko K. 2012. Empirical bayesian kriging. *ArcUser Fall.* **2012**: 6-10.

Landis J R, Koch G G. 1977. The measurement of observer agreement for categorical data. *Biometrics.* **33**: 159-174.

Leff B, Ramankutty N, Foley J A. 2004. Geographic distribution of major crops across the world. *Global Biogeochem Cycles.* **18**: GB1009.

Li B, Ti C, Yan X. 2020. Estimating rice paddy areas in china using multi-temporal cloud-free normalized difference vegetation index (ndvi) imagery based on change detection. *Pedosphere.* **30**: 734-746.

Li B, Ti C, Zhao Y, Yan X. 2016. Estimating soil moisture with landsat data and its application in extracting the spatial distribution of winter flooded paddies. *Remote Sens.* **8**: 38.

Liu L, Huang J, Xiong Q, Zhang H, Song P, Huang Y, Dou Y, Wang X. 2020. Optimal modis data processing for accurate multi-year paddy rice area mapping in china. *GIScience & Remote Sensing.* **57**: 687-703.

Liu R, Shang R, Liu Y, Lu X. 2017. Global evaluation of gap-filling approaches for seasonal ndvi with considering vegetation growth trajectory, protection of key point, noise resistance and curve stability. *Remote Sens Environ.* **189**: 164-179.

Lv T T, Liu C. 2010. Study on extraction of crop information using time-series modis data in the chao phraya basin of thailand. *Advances in Space Research.* **45**: 775-784.

Matthews E, Fung I, Lerner J. 1991. Methane emission from rice cultivation: Geographic and seasonal distribution of cultivated areas and emissions. *Global Biogeochem Cycles.* **5**: 3-24.

Munda G C, Das A, Patel D P. 2009. Evaluation of transplanted and ratoon crop for double cropping of rice (oryza sativa l.) under organic input management in mid altitude sub-tropical meghalaya. *Curr Sci.* **96**: 1620-1627.

NBS. 2016. China statistical yearbook 2015. (in Chinese.) China Statistical Press, Beijing.

Negalur R, Yadahalli G, Chittapur B, Guruprasad G, Narappa G. 2017. Ratoon rice: A climate and resource smart technology. *Int J Curr Microbiol App Sci.* **6**: 1638-1653.

Nelson G C, Rosegrant M W, Koo J, Robertson R, Sulser T, Zhu T, Ringler C, Msangi S, Palazzo A, Batka M. 2009. Climate change: Impact on agriculture and costs of adaptation. Intl Food Policy Res Inst.

Nocco M A, Smail R A, Kucharik C J. 2019. Observation of irrigation-induced climate change in the midwest united states. *Glob Chang Biol.* **25**: 3472-3484.

OCDE F. 2009. Oecd-fao agricultural outlook 2009-2018. Paris, OCDE. comptabilisée que pour la culture indiquée.

Olivier J G J, Bouwman A F, Berdowski J J M, Veldt C, Bloos J P J, Visschedijk A J H, van der Maas C W M, Zandveld P Y J. 1999. Sectoral emission inventories of greenhouse gases for 1990 on a per country basis as well as on 1°×1°. *Environmental Science & Policy.* **2**: 241-263.

Otsu N. 1979. A threshold selection method from gray-level histograms. *IEEE transactions on systems, man, and cybernetics.* **9**: 62-66.
Peng D, Huete A R, Huang J, Wang F, Sun H. 2011. Detection and estimation of mixed paddy rice cropping patterns with modis data. *Int J Appl Earth Obs Geoinf.* **13**: 13-23.
Peng S. 2014. Reflection on china's rice production strategies during the transition period. *SCIENTIA SINICA Vitae.* **44**: 845-850.
Sakamoto T, Yokozawa M, Toritani H, Shibayama M, Ishitsuka N, Ohno H. 2005. A crop phenology detection method using time-series modis data. *Remote Sens Environ.* **96**: 366-374.
Samsonova V P, Blagoveshchenskii Y N, Meshalkina Y L. 2017. Use of empirical bayesian kriging for revealing heterogeneities in the distribution of organic carbon on agricultural lands. *Eurasian Soil Sci.* **50**: 305-311.
Santos A B, Fageria N K, Prabhu A S. 2003. Rice ratooning management practices for higher yields. *Commun Soil Sci Plant Anal.* **34**: 881-918.
Silva D V S X D, Fernando W A C, Kodikaraarachchi H, Worrall S T, Kondoz A M. 2010. Adaptive sharpening of depth maps for 3d-tv. *Electron Lett.* **46**: 1546-1548.
Smil V. 1999. China's agricultural land. *The China Quarterly.* **158**: 414-429.
Sobrino J A, Julien Y. 2013. Trend analysis of global modis-terra vegetation indices and land surface temperature between 2000 and 2011. *IEEE J Sel Topics Appl Earth Observ Remote Sens.* **6**: 2139-2145.
Van Der Meer F, Bakker W. 1997. Ccsm: Cross correlogram spectral matching. *Int J Remote Sens.* **18**: 1197-1201.
van der Meero F, Bakker W. 1997. Cross correlogram spectral matching: Application to surface mineralogical mapping by using aviris data from cuprite, nevada. *Remote Sens Environ.* **61**: 371-382.
Wang J J, Lu X X. 2010. Estimation of suspended sediment concentrations using terra modis: An example from the lower yangtze river, china. *ScTEn.* **408**: 1131-1138.
Wardlow B D, Egbert S L. 2008. Large-area crop mapping using time-series modis 250 m ndvi data: An assessment for the us central great plains. *Remote Sens Environ.* **112**: 1096-1116.
White M A, de Beurs K M, Didan K, Inouye D W, Richardson A D, Jensen O P, O'Keefe J, Zhang G, Nemani R R, van Leeuwen W J D, Brown J F, de Wit A, Schaepman M, Lin X, Dettinger M, Bailey A S, Kimball J, Schwartz M D, Baldocchi D D, Lee J T, Lauenroth W K. 2009. Intercomparison, interpretation, and assessment of spring phenology in north america estimated from remote sensing for 1982-2006. *Glob Chang Biol.* **15**: 2335-2359.
Xiao X, Boles S, Frolking S, Li C, Babu J Y, Salas W, Moore III B. 2006. Mapping paddy rice agriculture in south and southeast asia using multi-temporal modis images. *Remote Sens Environ.* **100**: 95-113.
Xiao X, Boles S, Liu J, Zhuang D, Frolking S, Li C, Salas W, Moore III B. 2005. Mapping paddy rice agriculture in southern china using multi-temporal modis images. *Remote Sens Environ.* **95**: 480-492.
Yan X, Akiyama H, Yagi K, Akimoto H. 2009. Global estimations of the inventory and mitigation potential of methane emissions from rice cultivation conducted using the 2006 intergovernmental panel on climate change guidelines. *Global Biogeochem Cycles.* **23**: GB2002.
Yuan S, Cassman K G, Huang J, Peng S, Grassini P. 2019. Can ratoon cropping improve resource use efficiencies and profitability of rice in central china? *Field Crops Res.* **234**: 66-72.
Zhang F, Wang D, Qiu B. 1987. Agro-phenological atlas of china. (in Chinese.) Science Press, Beijing.

Zhang G, Xiao X, Dong J, Kou W, Jin C, Qin Y, Zhou Y, Wang J, Menarguez M A, Biradar C. 2015. Mapping paddy rice planting areas through time series analysis of modis land surface temperature and vegetation index data. *ISPRS J Photogramm Remote Sens.* **106**: 157-171.

Ziska L H, Fleisher D H, Linscombe S. 2018. Ratooning as an adaptive management tool for climatic change in rice systems along a north-south transect in the southern mississippi valley. *Agric For Meteorol.* **263**: 409-416.

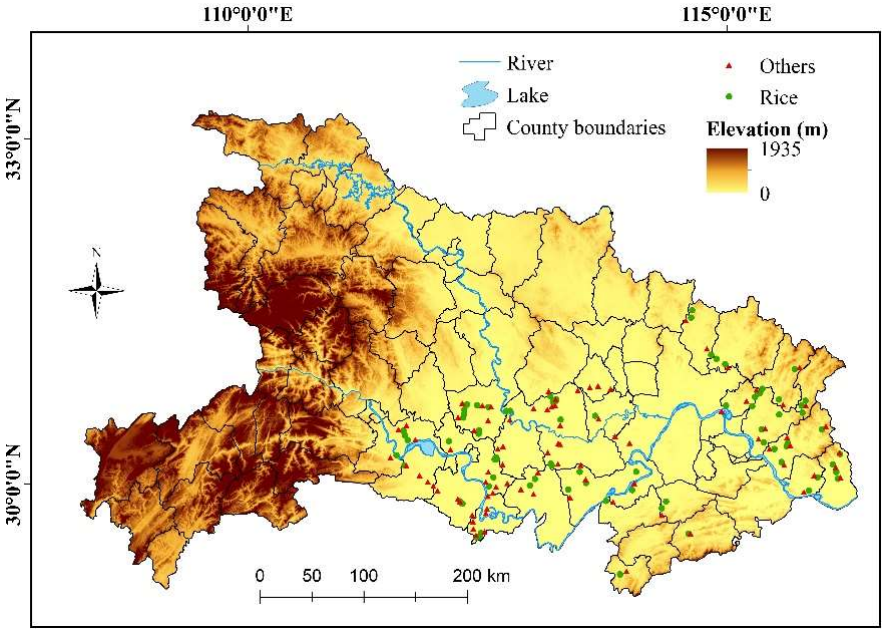
110°0'0"E
115°0'0"E
33°0'0"N
30°0'0"N
River
Lake
County boundaries
Others
Rice
Elevation (m)
1935
0
N
0 50 100 200 km

Fig. 1

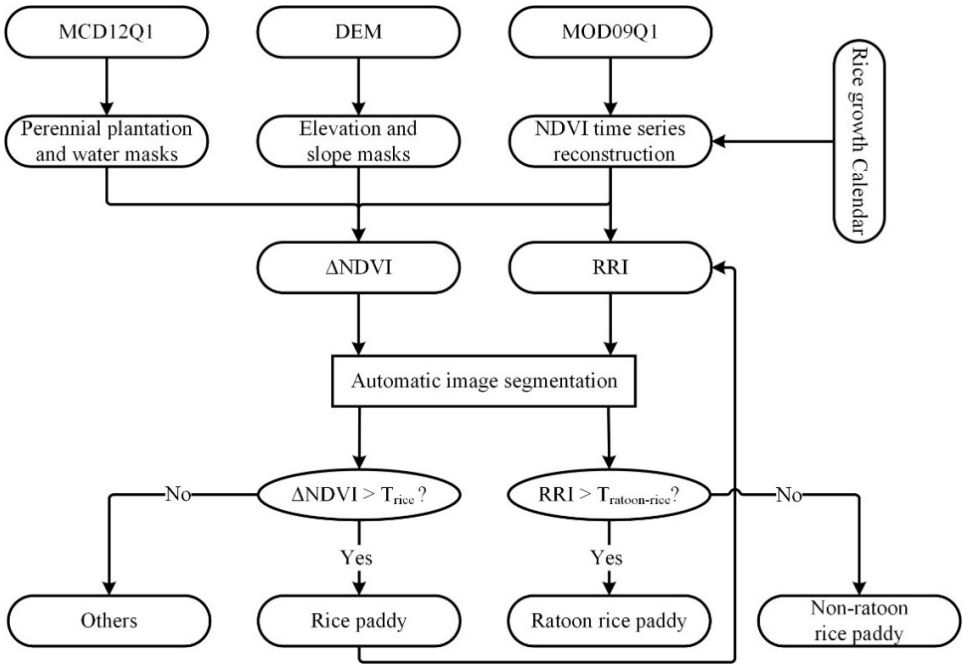
MCD12Q1
DEM
MOD09Q1
Rice growth Calendar
Perennial plantation and water masks
Elevation and slope masks
NDVI time series reconstruction
ΔNDVI
RRI
Automatic image segmentation
ΔNDVI > T_rice ?
RRI > T_ratoon-rice?
No
No
Yes
Yes
Others
Rice paddy
Ratoon rice paddy
Non-ratoon rice paddy

Fig. 2

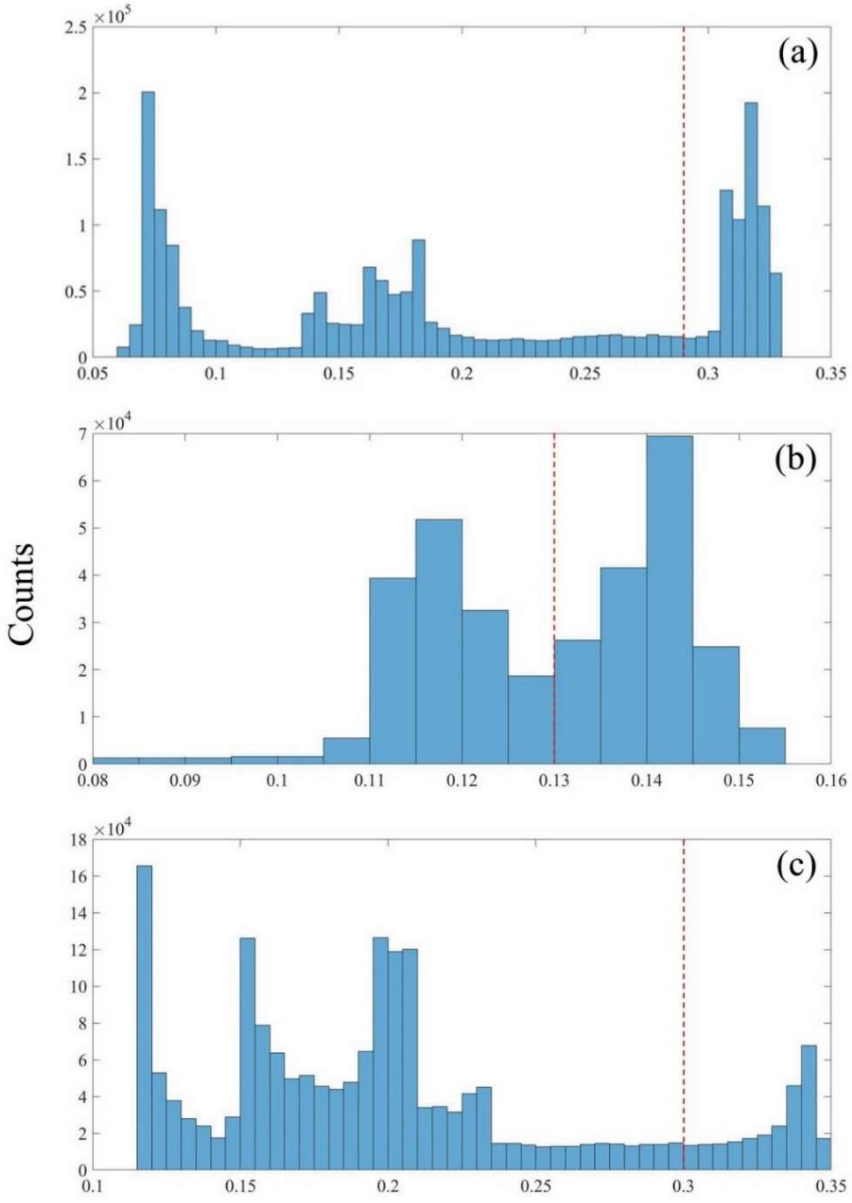

Fig. 3

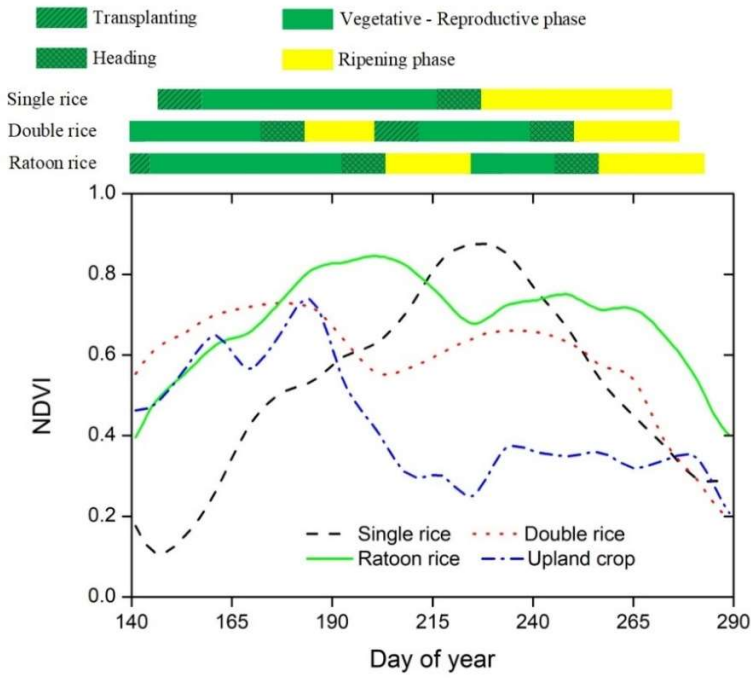
Transplanting
Vegetative - Reproductive phase
Heading
Ripening phase
Single rice
Double rice
Ratoon rice
NDVI
1.0
0.8
0.6
0.4
0.2
0.0
140
165
190
215
240
265
290
Day of year
Single rice
Double rice
Ratoon rice
Upland crop

Fig. 4

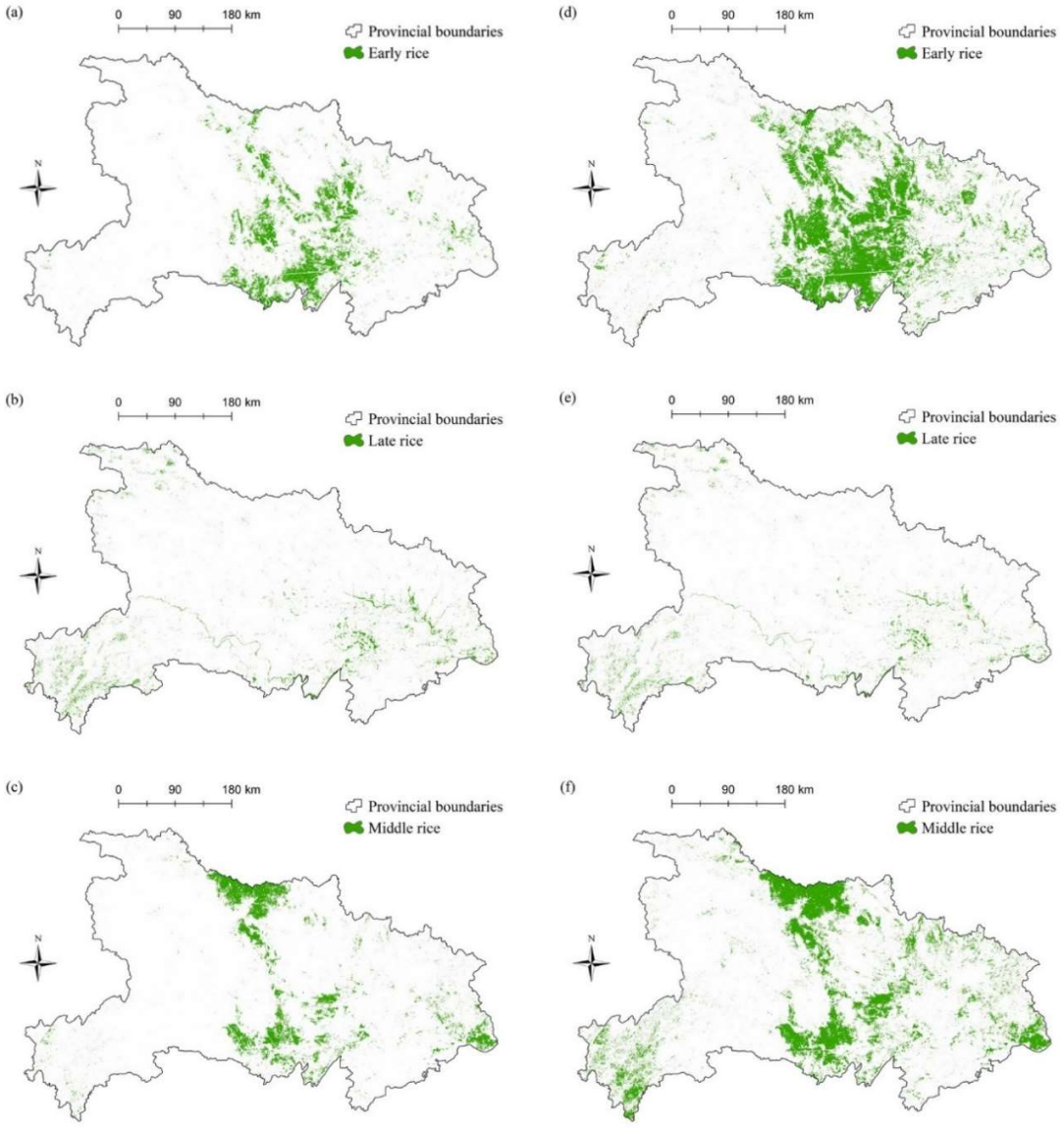
(a)
0 90 180 km
Provincial boundaries
Early rice
N
(d)
0 90 180 km
Provincial boundaries
Early rice
N
(b)
0 90 180 km
Provincial boundaries
Late rice
N
(e)
0 90 180 km
Provincial boundaries
Late rice
N
(c)
0 90 180 km
Provincial boundaries
Middle rice
N
(f)
0 90 180 km
Provincial boundaries
Middle rice
N

Fig. 5

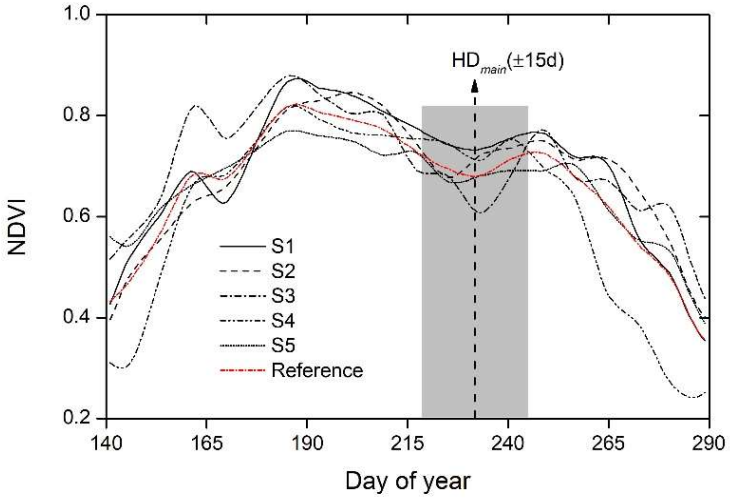
1.0
0.8
0.6
0.4
0.2
NDVI
HD$_{main}$(±15d)
S1
S2
S3
S4
S5
Reference
140
165
190
215
240
265
290
Day of year

Fig. 6

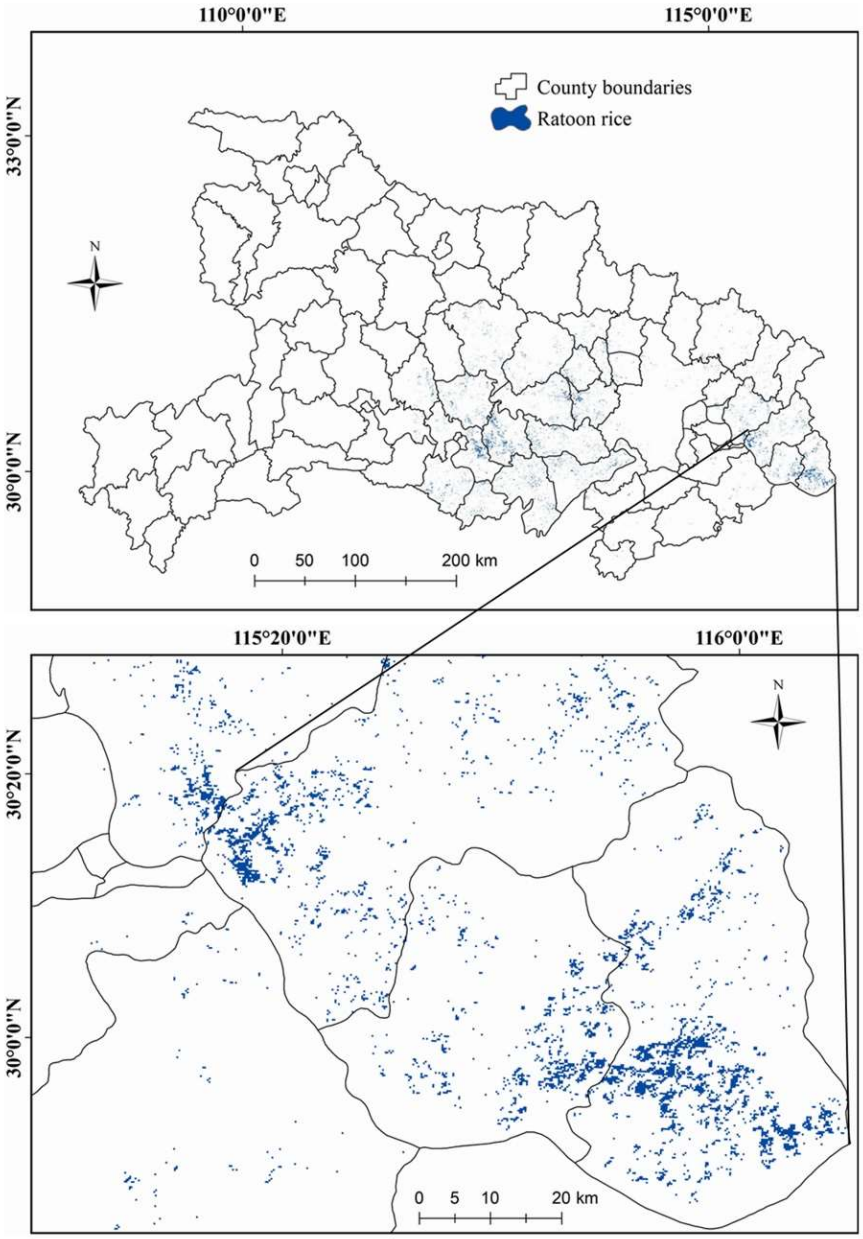
110°0'0"E
115°0'0"E
33°0'0"N
30°0'0"N
County boundaries
Ratoon rice
N
0 50 100 200 km
115°20'0"E
116°0'0"E
30°20'0"N
30°0'0"N
N
0 5 10 20 km

Fig. 7

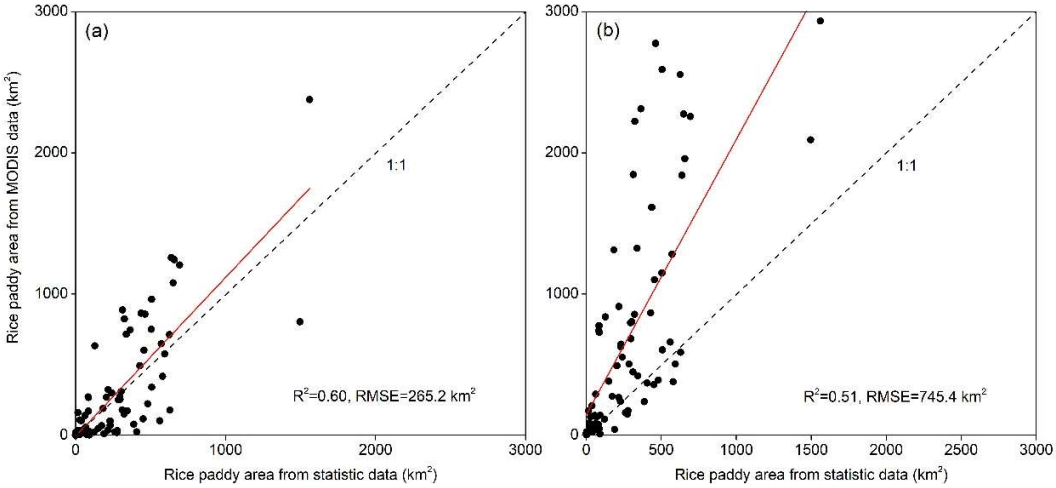
(a)
(b)
1:1
1:1
R²=0.60, RMSE=265.2 km²
R²=0.51, RMSE=745.4 km²
Rice paddy area from MODIS data (km²)
Rice paddy area from statistic data (km²)
Rice paddy area from statistic data (km²)
0
1000
2000
3000
500
1500
2500

Fig. 8

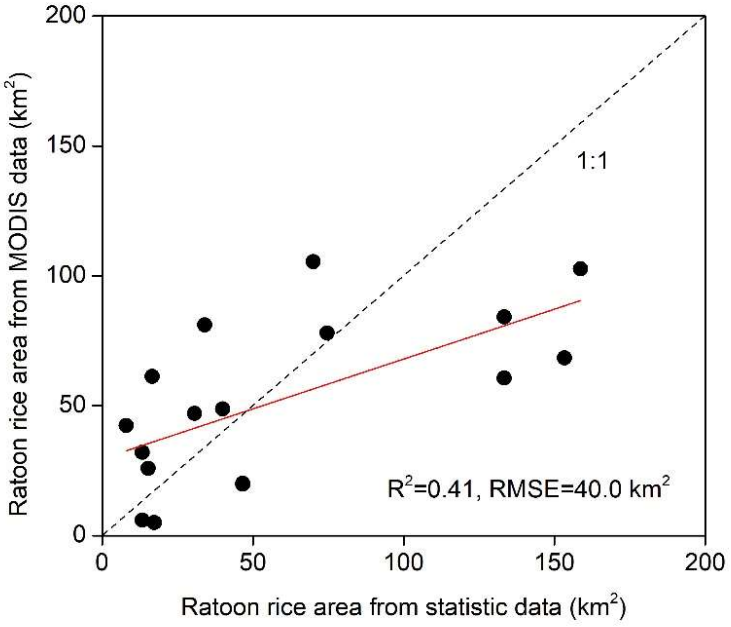
1:1
R²=0.41, RMSE=40.0 km²
Ratoon rice area from MODIS data (km²)
Ratoon rice area from statistic data (km²)
0
50
100
150
200

Fig. 9